

X-ray-diffraction and scanning-tunneling-microscopy studies of a liquid-crystal film adsorbed on single-crystal graphite

P. Dai, S.-K. Wang, H. Taub, and J. E. Buckley*

Department of Physics and Astronomy, University of Missouri-Columbia, Columbia, Missouri 65211

S. N. Ehrlich[†]

School of Materials Engineering, Purdue University, West Lafayette, Indiana 47907

J. Z. Larese

Brookhaven National Laboratory, Upton, New York 11973

G. Binnig and D. P. E. Smith

IBM Physics Group, Schellingstrasse 4, 8000 München, Germany

(Received 21 July 1992)

Synchrotron x-ray-diffraction and scanning-tunneling-microscopy (STM) experiments reveal a new commensurate monolayer structure of 10CB (decylcyanobiphenyl) molecules adsorbed on the (0001) graphite surface. Our results are consistent with two generic structures for n CB monolayers on surfaces of hexagonal symmetry. The monolayer d spacing of the new phase inferred by STM is 10% larger than that obtained by x-ray diffraction on the same sample. We suggest that part of this discrepancy results from a systematic error introduced in calibration of the STM length scale against the graphite substrate.

I. INTRODUCTION

Recently, there has been considerable activity in applying scanning tunneling microscopy (STM) to structure determinations of solid organic monolayers. Systems of particular interest include monolayers of molecules which have liquid-crystal phases in bulk such as the n -alkylcyanobiphenyls (n CB) but which form crystalline monolayers when adsorbed on various solid substrates.¹⁻⁴ One such system found to be especially favorable for investigation by STM and consequently one for which a detailed structural model has been developed is that of 10CB adsorbed on graphite.^{2,3} As shown in Figs. 1(a) and 1(c), the 10CB monolayer structure is commensurate with the graphite (0001) surface, consisting of double rows of molecules with five molecular pairs per unit cell.³

The 10CB monolayer structure inferred by STM is sufficiently complex (10 molecules per unit cell and 53 atoms per molecule) that one could not expect to solve it initially by x-ray surface diffraction techniques.⁵ Therefore, the original intent of the investigations reported here was to use x-ray diffraction to verify independently only some of its features. Surprisingly, both our STM and x-ray diffraction experiments have revealed a new commensurate monolayer structure for this molecule on graphite, one which is similar to that found for 8CB on an MoS₂ substrate. Thus our results provide evidence of two generic structures for n CB monolayers on surfaces of hexagonal symmetry. Below, we describe the new structure and demonstrate its stability well above the bulk 10CB smectic-to-isotropic fluid transition temperature.

In one case, we have been able to perform both STM and x-ray measurements on the *same* single-crystal sample and have found a 10% discrepancy in the monolayer d spacing inferred by the two techniques. We suggest that part of this discrepancy results from a systematic error introduced in calibration of the STM length scale against the graphite substrate.

STM has allowed structural features of the n CB monolayers to be determined, such as the number of molecules in the unit cell and their packing arrangement, which would be very difficult to establish by x-ray diffraction techniques alone. Nevertheless, surface x-ray diffraction has some advantages over STM in studies of film structure. Among these are the capability of scanning reciprocal space in a direction perpendicular to the adsorbing surface to yield details of the multilayer film structure and its thickness which are inaccessible to STM. In addition, the relatively high resolution of x-ray scans parallel to the surface enables determination of the average monolayer d spacings with a precision at least an order of magnitude greater than by STM. X-ray diffraction can also be used to characterize the short-range order in fluid films where increased mobility of the molecules may result in a complete loss of the STM image. Another advantage of x-ray scattering is the ease of investigating film structures at elevated temperatures. With x-ray diffraction, one might also hope to address the question of whether the STM technique perturbs the structure of the film or substrate under investigation (e.g., by means of applied voltage pulses or by movement of the probe through the film). The experiments reported here are, to our knowledge, the first in which both STM and x-ray methods have been applied to the same sample of an organic film.

II. EXPERIMENTAL TECHNIQUE

In this study, both single crystals and highly oriented pyrolytic graphite (HOPG) were used as substrates. The single crystals had surface diameters of 1.5–3 mm and were ~ 0.1 mm thick, while the HOPG samples had surface dimensions of 6×6 mm and were 1 mm thick. The substrates were epoxied on an aluminum pedestal which could be mounted either on an STM unit or any x-ray goniometer. Film growth was either by vapor deposition² or melting of a small 10CB grain.³

It should be emphasized that sample requirements for an x-ray diffraction experiment are much more stringent than for STM. With STM one can image single domains of the 10CB monolayer with atomic resolution. The STM images presented here had fields of view ranging

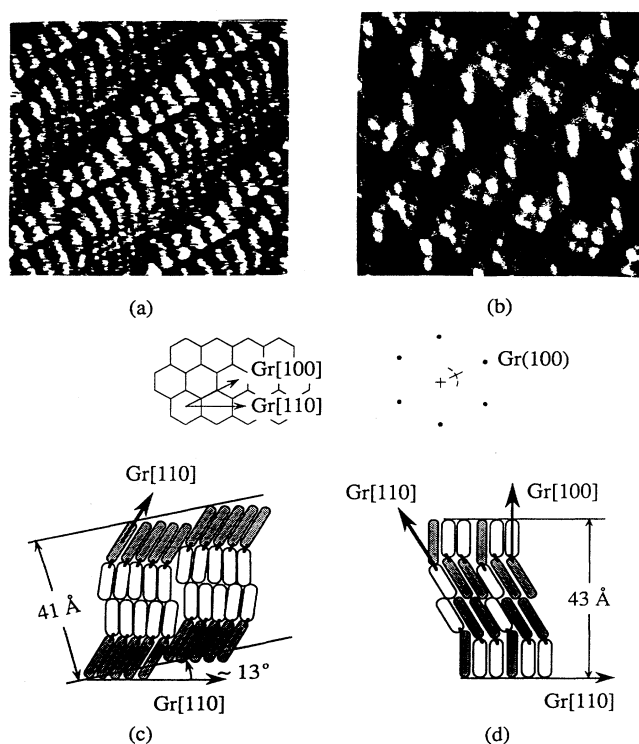


FIG. 1. Constant-current STM images of the S1 and S2 monolayer phases of 10CB on the (0001) surface of highly oriented pyrolytic graphite (HOPG) and their corresponding models: (a) $100 \times 100 \text{ \AA}^2$ image of the S1 phase taken using a cut Pt/Ir STM tip, a tunnel current equal to 90 pA, and a bias voltage equal to 933 mV (tip negative). The double-row spacing of 41 Å obtained by calibration against the graphite substrate is approximately 5% less than that reported in Ref. 3; (b) $75 \times 75 \text{ \AA}^2$ image of the S2 phase taken using an electrochemically etched tungsten tip, tunnel current equal to 100 pA, and bias voltage equal to 1.1 V (tip negative). (c) Model of the S1 phase (from Refs. 2 and 3). For each molecule, the shaded and open regions represent the alkyl tail and head group, respectively. (d) Model of the S2 phase. The schematic models in (c) and (d) do not accurately depict the interdigitation of the cyano head groups believed to be present in both phases. Insets define interdigitation directions in the graphite basal plane in real space (left) and in reciprocal space (right).

from $75 \times 75 \text{ \AA}^2$ to $480 \times 480 \text{ \AA}^2$. In x-ray experiments, on the other hand, even utilizing synchrotron sources, there is insufficient intensity to observe diffraction from single monolayer domains of dimension $\sim 1000 \text{ \AA}$. In particular, we were unable to observe Bragg peaks from 10CB films adsorbed on HOPG substrates in scans parallel to the surface even though these samples had yielded good quality STM images of the 10CB monolayer. Presumably, this is due to the random in-plane orientation of the HOPG graphite crystallites which spreads the Bragg reflections from the film into rings of scattering whose intensity is too weak to be observed.

The x-ray experiments require samples with preferential orientation of domains over an area on the order of the x-ray beam size ($\sim 1 \text{ mm}^2$). The only case in which we achieved this and were able to observe a Bragg peak from a 10CB monolayer was for a sample grown on a single-crystal graphite substrate. Due to the weakness of the scattering, the x-ray beam could not be reduced in size to probe diffraction from different regions of this sample. Unfortunately, attempts at observing a monolayer Bragg peak with other single-crystal supported samples were unsuccessful. Since the number, size, and orientational distribution of the 10CB domains could not be determined from the STM images, it was impossible to use STM to select favorable samples for the x-ray experiments.

The x-ray experiments were performed at the x18A beam line at the National Synchrotron Light Source using a double (flat) Si(111) monochromator set at a wavelength of 1.56 Å. A bent platinum-coated mirror was used to focus the x-ray beam vertically and horizontally. Using a slit in front of the detector to define the scattered beam, we obtained longitudinal and transverse resolution widths (full width at half maximum) of $6.6 \times 10^{-3} \text{ \AA}^{-1}$ and $1.3 \times 10^{-4} \text{ \AA}^{-1}$, respectively, for in-plane scans of the monolayer Bragg peak.

III. RESULTS

A. STM

With both HOPG and single-crystal substrates we were able to obtain good quality STM images of the 10CB monolayer structure found previously by Smith *et al.*^{2,3} (hereafter referred to as the S1 structure) as shown in Fig. 1(a).⁶ However, one of the single-crystal samples showed evidence of a new structure, denoted S2, in which the molecules are again arranged in double rows but without a lateral shift every five molecular pairs. STM images of the S2 structure having higher spatial resolution were later obtained from HOPG-supported films as shown in Fig. 1(b).⁷ Within each row, one sees a periodic variation of intensity every third molecule. Associating the brightest part of the molecule with the head group,^{2,3} we interpret the image as shown schematically in Fig. 1(d) where every third molecule in a row has been reversed head for tail. The S2 phase preserves the double-row periodicity of the S1 structure in which adjacent rows meet head-to-head and tail-to-tail.

In the case where we observed the S2 monolayer on the

single-crystal substrate, we were able to calibrate the length scale in the film images by driving the STM probe closer to the substrate to image the underlying graphite plane.³ In this way, the S2 double-row d spacing was measured to be 43 Å. The analysis also gave the orientation of the monolayer “director” (the unit vector parallel to graphite surface and perpendicular to the double rows of molecules) as nearly along the graphite [100] direction.

The S2 structure is similar to that found by Hara *et al.*⁸ for 8CB on MoS₂ except that in their structure every other molecule within a row is reversed. We note that, on the graphite (0001) surface, 8CB also has a structure similar to the S1 phase of 10CB [see Fig. 1(a)] except that it has four molecular pairs in a unit cell.^{3,8} Thus both 8CB and 10CB when adsorbed on hexagonal surfaces exhibit two generic monolayer structures: one in which all molecules within a row point in the same direction but in which a periodic lateral shift occurs as one moves along a row, and another in which there is no lateral shift but in which molecules are periodically reversed in direction along a row.

Although growth of a particular phase is not generally predictable,⁷ the two phases have been grown on both single-crystal and HOPG substrates and by both vapor deposition² and melted grain methods.³ We assume that the S1 phase is more energetically stable at room temperature since it is much more frequently observed. It is unclear at the present time what determines the appearance of one or the other structure; and, in fact, both phases can exist on the *same* sample under apparently identical conditions. Figures 2(a) and 2(b) show STM images of two regions of the same HOPG separated by a few hun-

dred nanometers, one area having molecules arranged in the S1 structure and the other in the S2 structure. The two regions are divided by a disordered boundary in the HOPG substrate, presumably the boundary between neighboring graphite crystallites.

Coexistence of the S1 and S2 phases on the same crystallite is shown in the STM image of Fig. 2(c) taken on another HOPG-supported sample. The angle between directors of the two phases is measured to be 12°, consistent with the 13° angle between S1 rows and the graphite [110] direction shown in the schematic of Fig. 1(c). At times, the S1-S2 boundary was slightly blurred, which may indicate molecular motion at the interface (the acquisition time for one image was about 10 s). In other examples of coexisting S1 and S2 phases, the interface was quite fluid and could be seen to move back and forth several nanometers on the time scale of a few minutes. Dynamical behavior of this sort has been reported by Rabe and Buchholz for didodecylbenzene⁹ and octadecanol¹⁰ on HOPG. We do not believe that a first-order transition occurs between these phases because, as shown below, the S2 structure is stable over a wide temperature range.

B. X-ray diffraction

At the time of our x-ray experiments, we had only obtained STM images of the S1 phase from HOPG-supported films.⁶ As noted earlier, there was insufficient intensity to observe in-plane Bragg peaks from films on these substrates. However, we were successful in such measurements using the *same* single-crystal sample from which we obtained the first STM images of the new S2 structure. This sample was prepared by the vapor deposition method as in previous experiments.² The x-ray measurements were greatly facilitated by knowing that the monolayer director was close to the graphite [100] direction as determined from the Fourier transforms of the monolayer and graphite STM images. As shown in Fig. 3, we found a Bragg peak of the monolayer in a radial scan parallel to the surface at an azimuth of $\sim 0.6^\circ$ away from the graphite [100] direction. We emphasize that this direction is different from that expected for the S1 structure.³ From Fig. 1(c) (see also Fig. 2 in Ref. 3), it can be seen that the Bragg peak corresponding to the double-row periodicity of the S1 monolayer would be $\sim 13^\circ$ away from the graphite [110] direction.

There are two features of the x-ray diffraction scans which are consistent with the S2 monolayer phase being commensurate with the graphite (0001) surface as suggested by the STM measurements. First, we observed a similar Bragg peak in an in-plane scan directed 60° away from the first one. Since the STM images of the S2 phase do not have hexagonal symmetry, we conclude that this peak is contributed by other domains of the S2 commensurate monolayer on the same graphite crystallite. Second, the d spacing inferred from the position of both peaks is 38.3 Å or $9\sqrt{3}a_0$ where $a_0 = 2.46$ Å is the lattice constant in the graphite basal plane. As will be discussed below, this d spacing is about 10% less than the value of 43 Å inferred by STM.

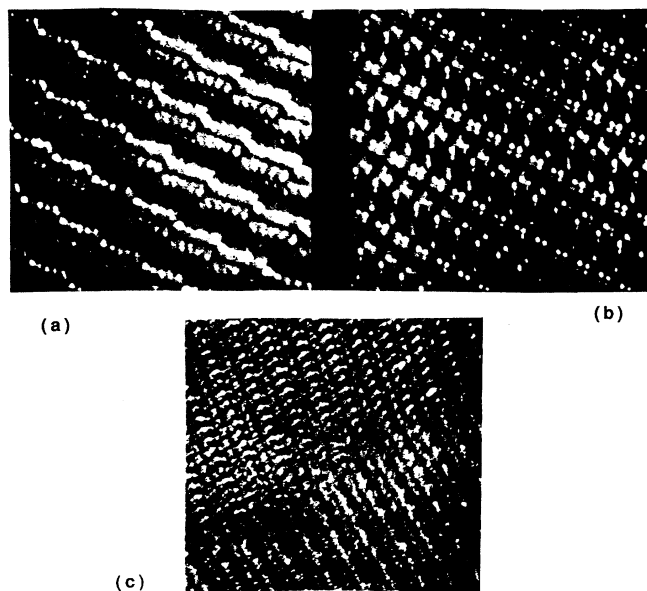


FIG. 2. STM images of the S1 and S2 phases coexisting on the same HOPG sample. (a) S1 phase (240×240 Å²) and (b) S2 phase (180×180 Å²) separated by a graphite grain boundary (not shown). (c) S1 phase (bottom) and S2 phase (top) meeting at a molecularly defined interface (480×480 Å²). The imaging conditions were the same as in Fig. 1(b).

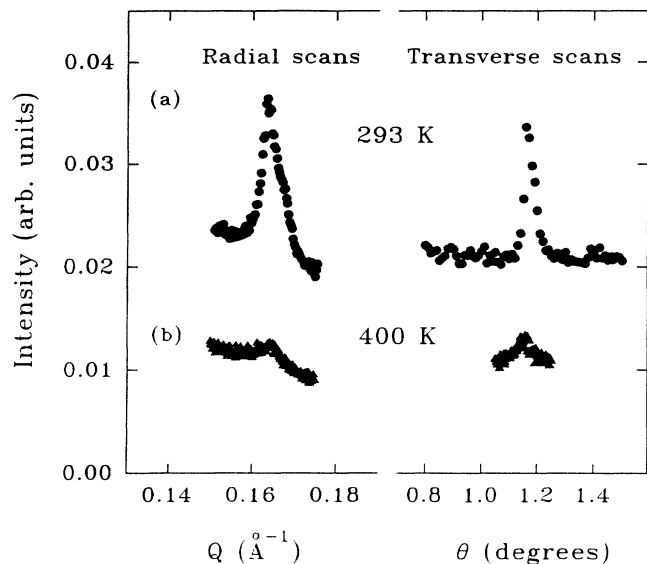


FIG. 3. In-plane x-ray scans through the Bragg peak of the S2 monolayer phase of 10CB in the radial (left panel) and transverse (right panel) directions at temperatures of (a) 293 K and (b) 400 K. The scan directions are indicated schematically in the right-hand inset to Fig. 1: radial (solid line) and transverse (dashed arc). In the transverse scans, the graphite (100) peak occurs at $\theta=0.55^\circ$.

We were also able to investigate the stability of the 10CB monolayer by x-ray diffraction above room temperature. It can be seen in Fig. 3 that the monolayer Bragg peak weakens upon heating to 400 K. Since the sample was heated in a vacuum enclosure, this could be the result of film desorption. It might also be due to the effect of a Debye-Waller factor. We note that there is no measurable shift in the peak position, indicating the absence of thermal expansion as might be expected for a commensurate structure. At both temperatures, the width of the Bragg peak is limited by the instrumental resolution which gives a lower bound on the monolayer coherence length of ~ 900 Å. From these measurements, we conclude that the film has not melted at 400 K and hence is remarkably stable compared to those of shorter alkane molecules on graphite.¹¹

IV. DISCUSSION

The 10% discrepancy between the monolayer double-row d spacing of 38.3 Å inferred by x-ray diffraction and the value of ~ 43 Å determined by STM is about twice the estimated uncertainty based on the reproducibility of the STM measurements.³ We have considered several different explanations for this discrepancy. A possible source of error in the x-ray determination is associated with the small asymmetry of the Bragg peak which appears in the radial but not the transverse direction (see Fig. 3). This may be due to the out-of-plane mosaic of the graphite substrate which gives a “sawtooth” Warren line shape¹² to the peak as in experiments using exfoliated graphite substrates.¹¹ For a finite-size sample, the peak in the Warren line shape is displaced to a Q value greater

than $2\pi/d$. Using an expression for this shift derived in Warren’s paper¹² and assuming a monolayer coherence length of ≥ 900 Å, we calculate that this effect would increase the d spacing by $\leq 1.5\%$ from its value of 38.3 Å.

Another possible explanation of the discrepancy between the STM and x-ray d spacings of the S2 structure which we have considered involves packing faults within the monolayer such as a missing row. Estimates from model calculations suggest that a 10% outward shift in the peak position would require a missing row to occur in every three double rows. However, such a fault density should have been observable in the STM images which were taken with fields as large as 3000 Å.

Yet another possibility which we have considered is that x rays are sampling a periodicity associated with a multilayer commensurate film which may be shorter than that of the first layer imaged by STM. We investigated the multilayer structure of this sample by performing a room-temperature diffraction scan along the (10) Bragg rod of the 10CB film (parallel to the surface normal) at fixed $Q_{\parallel}=2\pi/38.3$ Å⁻¹. The direction of the incident x-ray beam was held fixed parallel to the graphite surface. This scan is shown in Fig. 4. The pronounced peak at $Q_{\perp}\approx 0.01$ Å⁻¹ occurs when the exit beam leaves the graphite surface at the critical angle for the 10CB film ($\sim 0.14^\circ$) so that the incident and total reflected wave are in phase.⁵ In principle, this should lead to an enhancement of the scattered intensity by a factor of 4; however, the effects of absorption and surface mosaic reduce this enhancement. Due to uncertainties in estimating the latter two effects, we have not tried to analyze this region of the scan quantitatively.

The solid curve in Fig. 4 is the rod profile calculated for a single layer of the S2 phase as shown in the model of Fig. 1(d). The monotonic decrease in intensity results

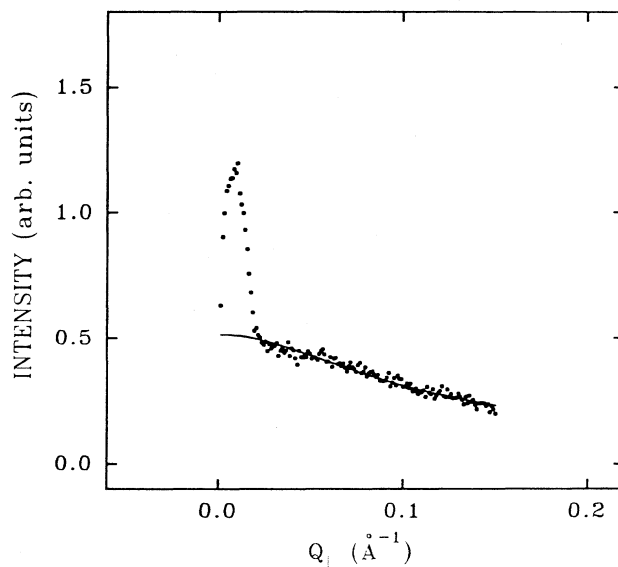


FIG. 4. Out-of-plane x-ray scan at 294 K through the same Bragg peak of the S2 phase as in Fig. 3. The solid line is calculated as described in the text.

from the effect of instrumental resolution which has been approximated using the method developed by Robinson^{13,14} for a rod scan. The calculated profile is normalized to the intensity at $Q_{\perp}=0.025 \text{ \AA}^{-1}$ just beyond the region of enhancement. At higher Q_{\perp} , the observed scattering profile is in good agreement with the curve calculated for the 10CB monolayer. We note that a similar curve has been both observed and calculated for the (10) rod of a Xe monolayer on graphite.¹⁵

We also measured the specular x-ray reflectivity from the sample exhibiting the S2 structure in its STM image. In this measurement, one again scans Q_{\perp} but at a fixed $Q_{\parallel}=0$. As can be seen in Fig. 5, the reflectivity is featureless, having the same monotonic decrease with Q_{\perp} which we observed from bare graphite substrates as shown in Fig. 6(a). Comparing the specular reflectivity of a similarly vapor-deposited film on an HOPG substrate in Fig. 6(b) suggests that the HOPG-supported film is thicker. The latter shows weak intensity undulations in its reflectivity characteristic of a multilayer film. Also, at higher Q_{\perp} (not shown), weak peaks from bulk crystalline 10CB appear.¹⁶ We interpret this behavior as indicating coexistence of a solid multilayer 10CB film with bulk crystalline 10CB particles on the graphite surface. Above the bulk crystalline-to-smectic-*A* transition at 317 K, the intensity undulations due to the film shift in position and become stronger as shown in Fig. 6(c) and the bulk peaks disappear. We conclude that, at this temperature, complete wetting of the 10CB film to the HOPG substrate has occurred. Analysis of the reflectivity curves in Figs. 6(b) and 6(c) based on a simple model of a film of uniform charge density, shows the film thickness to increase from $\sim 45 \text{ \AA}$ at room temperature to $\sim 100 \text{ \AA}$ at 317 K.¹⁷

In addition to the sample of Fig. 6, all others made either by the same vapor deposition method or by melting

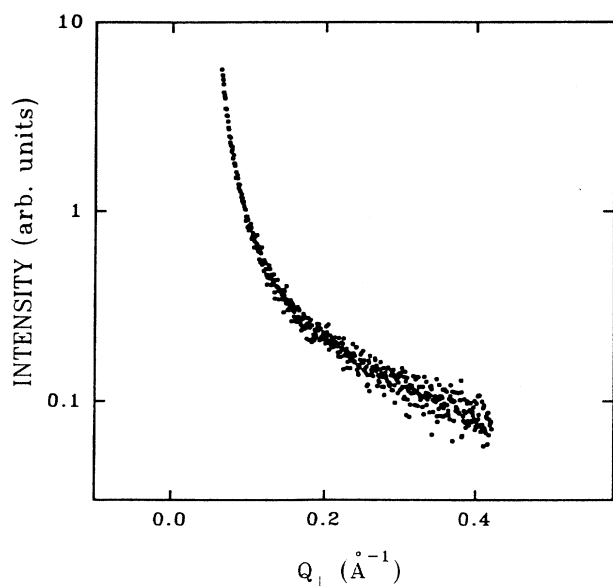


FIG. 5. Specular reflectivity x-ray scan from the sample exhibiting the S2 monolayer phase.

a grain of 10CB on the graphite surface resulted in the growth of a thicker film than the S2 sample of Figs. 3–5. The thickest polycrystalline 10CB films were obtained by the melted grain method, but these appeared to have a different structure than either the S1 and S2 monolayer phases. With these samples, a Bragg peak corresponding to a d spacing of $\sim 36 \text{ \AA}$ was observed in scans both parallel and perpendicular to the graphite surface with the peak in the latter scans being much more intense. We interpret this behavior as resulting from a polycrystalline film in which most of the molecules were oriented with their long axis *perpendicular* to the surface.^{17,18}

To summarize, the out-of-plane x-ray scans in Figs. 4 and 5 are consistent with a film of monolayer thickness.

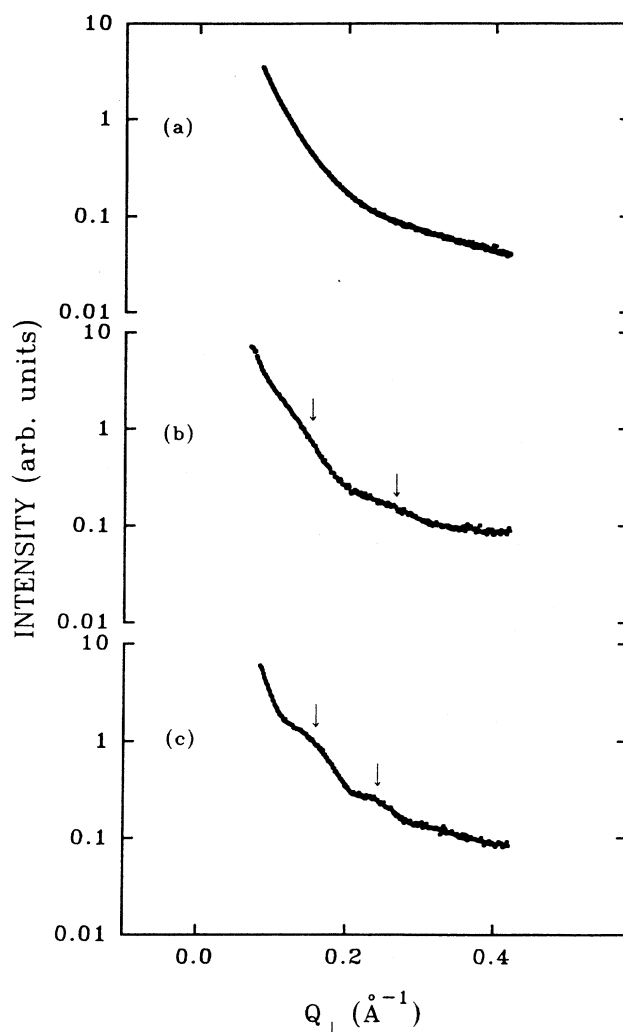


FIG. 6. Specular reflectivity x-ray scans from an HOPG-supported sample. (a) Bare HOPG substrate. (b) Same substrate at room temperature after 30-min deposition of 10CB. Arrows mark reflectivity changes due to the 10CB film. (c) Same as in (b) except sample temperature is 317 K. Note that reflectivity changes due to the 10CB film are enhanced and shifted in position compared to those at room temperature, indicating a thicker film.

The rod scan agrees quantitatively with that calculated for a monolayer above the critical angle for the exit beam, and the specular reflectivity does not show undulations characteristic of thicker films. It is difficult to explain why vapor deposition resulted in monolayer coverage for this sample. As noted earlier,⁷ this growth process is poorly controlled while the single-crystal substrates vary in size and quality.

In comparing our best STM images of the S1 phase from different samples, we found that the ratio of two distances within an image, the double-row spacing to the separation of adjacent alkyl tails, was generally more reproducible than the value of the double-row spacing obtained by calibration against the graphite substrate. This led us to consider the possibility that the discrepancy in the measured STM and x-ray d spacings results from a systematic error introduced in using the graphite substrate to calibrate the STM length scale.

Although we do not have an independent calibration method in the STM experiment, there is strong, albeit indirect, evidence that the lateral separation of adjacent alkyl tails of the 10CB molecules in the S1 phase is exactly 4.26 Å due to their registry with the graphite substrate [see Fig. 2(b) in Ref. 3]. This evidence is summarized in Ref. 3 and includes (a) alignment of the tails along the graphite [110] directions as determined by STM [see Fig. 1(c)]; (b) a similar registry effect inferred by STM for n -alkane molecules on graphite,^{10,19,20} and (c) consistency with potential-energy calculations for single alkane molecules on graphite.²¹

Assuming the tail-tail spacing in the S1 phase to be 4.26 Å, we can scale to this distance in the STM image of Fig. 1(a) to obtain an S1 double-row d spacing which is about 10% smaller than that found by the graphite calibration method [Fig. 1(c)]. Then using the coexistence of the S1 and S2 phases in the STM image of Fig. 2(c), we estimate a double-row spacing of 40 Å for the S2 structure. This is equal to the value of 38.3 Å inferred by x-ray diffraction to within the 5% reproducibility of the STM measurement.

Although the origin of the systematic error in the graphite calibration remains uncertain, it may result from frictional effects as the STM probe pierces the monolayer film. For example, embedding the probe in the 10CB film may exert a frictional force opposing the motion of the tip. A larger piezovoltage would then be required to scan the tip over a given number of carbon atoms in the graphite basal plane compared to that for a bare surface. Since a larger voltage is read as a larger distance, this would be consistent with the greater d spacing which we have found by STM than by x-ray diffraction. One might hope to test for this frictional effect by comparing the applied piezovoltage for a given excursion on bare graphite with the same excursion on graphite covered by film. Unfortunately, such a test is difficult due to the problem of controlling all other experimental parameters (tip condition, thermal effects, graphite quality, etc.).

Assuming the x-ray determination of the double-row spacing in the S2 phase to be correct, we conclude that there is a greater degree of interdigitation of the cyano head groups in the S2 phase than inferred previously for

the S1 structure.³ We do not believe this possibility is excluded by the STM measurements. The S1 and S2 images in Figs. 1(a) and 1(b), respectively, as well as those in Figs. 2(a) and 2(b) do not allow a quantitative determination of the interdigitation present in the two phases.

V. CONCLUSION

We have found a new, stable, commensurate monolayer structure for 10CB films adsorbed on a graphite basal plane surface which is similar to that observed for 8CB on MoS₂. Our results provide evidence of two generic crystalline structures of n CB monolayers on hexagonal surfaces.

We find that the monolayer d spacing of the new phase (S2) inferred by STM is 10% larger than that obtained by x-ray diffraction on the same sample. However, both probes yield the same orientation of the lattice vectors of the S2 phase with respect to those of graphite. Moreover, x-ray diffraction scans on this sample perpendicular to the graphite surface are consistent with a film of monolayer thickness. Thus there is strong evidence that both the STM and x-ray techniques are probing the same 10CB monolayer film.

After considering a number of alternative explanations, we suggest that the discrepancy in the S2 monolayer d spacing measured by the two techniques is most plausibly explained by including a systematic error in the calibration of the STM length scale against the graphite substrate. While the calibration procedure is reproducible at about the 5% level, our x-ray measurements indicate that there is an additional $\sim 5\%$ systematic error which may be caused by frictional effects of the monolayer on the STM probe when the graphite substrate is imaged. It would clearly be desirable to substantiate the presence of a systematic error with x-ray measurements on other single-crystal-supported films including samples of the S1 phase. Obtaining additional samples will require a major effort to control film growth conditions such as using ultrahigh vacuum techniques. Nevertheless, for the sample investigated here, both in-plane and out-of-plane x-ray diffraction results are consistent with a systematic error introduced in the STM calibration procedure.

These experiments demonstrate the complementary nature of the two techniques for monolayer structure determinations: the application of STM to infer qualitative features of the molecular packing and orientational order and the use of x-ray diffraction to obtain precise structural parameters over a wide temperature range. Together they strongly motivate theoretical efforts to understand the intermolecular and molecule-substrate interactions which stabilize the two classes of structures observed in n CB monolayers.

ACKNOWLEDGMENTS

The authors are indebted to P. Pfeifer who encouraged collaboration on this project, to G. P. Felcher who provided the graphite single crystals, and to H. W. White for the use of his STM apparatus on which some of the mea-

surements were performed. Many helpful discussions with L. B. Sorensen and J. Wragg are gratefully acknowledged. This work was partially supported by U.S. National Science Foundation Grants Nos. DMR-8704938

and DMR-9011069 (H.T.), U.S. Department of Energy Grant No. DE-FG02-85ER45183 (S.N.E. and H.T.), and U.S. Department of Energy Contract No. DE-AC02-76CH00016 (J.Z.L.).

*Present address: Department of Physics and Astronomy, University of Kansas, Lawrence, KS 66045.

†Present address: NSLS, Brookhaven National Laboratory, Upton, NY 11973.

¹J. S. Foster and J. E. Frommer, *Nature* **333**, 542 (1988).

²D. P. E. Smith, H. Hörber, Ch. Gerber, and G. Binnig, *Science* **245**, 43 (1989).

³D. P. E. Smith, J. K. H. Hörber, G. Binnig, and H. Nejh, *Nature* **344**, 641 (1990).

⁴D. P. E. Smith and J. E. Frommer, in *STM and SFM in Biology*, edited by O. Marti and M. Amrein (Academic, London, 1993), and references cited therein.

⁵See, for example, R. Feidenhans'l, *Surf. Sci. Rep.* **10**, 105 (1989).

⁶At the time of our x-ray experiments (see below), we had only obtained STM images of the S1 phase on HOPG substrates. Subsequently, S1 images were obtained using single-crystal substrates.

⁷These images were obtained after completion of the x-ray experiments from films prepared by the melted grain method. Attempts at growing the S2 phase on single-crystal substrates at this time were unsuccessful. While this history demonstrates that growth of both the S1 and S2 phases was reproducible, it emphasizes the difficulty of growing them predictably by the vapor deposition and melted grain methods. Similar problems related to controlling growth conditions are reported for alkane films in Ref. 20.

⁸M. Hara, Y. Iwakabe, K. Tochigi, H. Sasabe, A. F. Garito, and A. Yamada, *Nature* **344**, 228 (1990).

⁹J. P. Rabe and S. Buchholz, *Phys. Rev. Lett.* **66**, 2096 (1991).

¹⁰J. P. Rabe and S. Buchholz, *Science* **253**, 424 (1991).

¹¹H. Taub, in *The Time Domain in Surface and Structural Dynamics*, Vol. 228 of *NATO Advanced Study Institute, Series C: Mathematical and Physical Sciences*, edited by G. J. Long and F. Grandjean (Kluwer, Dordrecht, 1988), p. 467.

¹²B. E. Warren, *Phys. Rev.* **59**, 693 (1941).

¹³I. K. Robinson, *Aust. J. Phys.* **41**, 359 (1988).

¹⁴The out-of-plane resolution at $Q_{\perp}=0$ is 0.014 \AA^{-1} (full width at half maximum).

¹⁵H. Hong and R. J. Birgeneau, *Z. Phys. B* **77**, 413 (1989).

¹⁶The peak positions are in agreement with those which we have observed from a bulk powder of 10CB. A structure determination has recently been made for the bulk crystalline phase of 10CB: C. Barnes and E. L. Schlemper (private communication).

¹⁷P. Dai, S.-K. Wang, H. Taub, S. N. Ehrlich, and J. Z. Larese (unpublished).

¹⁸A similar picture has emerged in very recent molecular-dynamics simulations of liquid multilayer films of hexadecane ($C_{16}H_{34}$) adsorbed on a solid surface: T. K. Xia, J. Ouyang, M. W. Ribarsky, and U. Landman, *Phys. Rev. Lett.* **69**, 1967 (1992). The simulations show a tendency for the flexible alkane molecules to align with their long axis perpendicular to the substrate at coverages above monolayer completion. In the first layer, the molecules lie with their long axis parallel to the surface as we have found for both the S1 and S2 monolayer phases of 10CB on graphite. Although the simulations are done for a liquid film of pure alkane molecules, it is not unreasonable to expect this type of orientational order to be present in solid as well as liquid *n*CB films in which the molecules have a long alkyl tail.

¹⁹The repeat unit in the graphite basal plane perpendicular to the [110] direction is 4.26 \AA . It is conceivable that the tails are not spaced at this distance but at some rational multiple of it so that every *n*th molecule is in registry with the graphite surface. However, this is not the case with alkane molecules which have the same width as the alkyl tail in 10CB. Rabe and Buchholz (Ref. 10) were able to image an alkane monolayer and graphite substrate simultaneously and found no discernible superstructure thereby concluding commensurability with a repeat unit of 4.26 \AA .

²⁰G. C. McGonigal, R. H. Bernhardt, and D. J. Thomson, *Appl. Phys. Lett.* **57**, 28 (1990).

²¹F. Y. Hansen and H. Taub, *Phys. Rev. B* **19**, 6542 (1979).